International Journal of Thermophysics, Vol. 27, No. 2, March 2006 (© 2006)
DOI: 10.1007/s10765-005-0009-y

Spectral-Directional Emittance of 99.99% Aluminum, Thermally Oxidized Below Its Melting Point

G. Teodorescu,[1,2] P. D. Jones,[1] R. A. Overfelt,[1] and B. Guo[1]

Received April 4, 2005

Spectral-directional emittance measurements for 99.99% aluminum, thermally oxidized in air, were performed using a radiometric technique. The apparatus is comprised of a Fourier transform infrared spectrometer and a blackbody-radiating cavity. The sample holder is held on a slotted arc rack, which allows directional measurements from normal to grazing angles. The aluminum sample was heated for an extended period of time (150 h) at high temperature below its melting point prior to performing measurements. The data presented here cover the spectral range between 3 and 14 μm, directional range from surface normal to 72° polar angle, and temperatures from 673 to 873 K. The complex index of refraction is also reduced from emittance data. Auger electron spectroscopy (AES), X-ray photoelectron spectroscopy (XPS), and Auger depth profiling were used as surface techniques to characterize the thickness and composition of aluminum oxide film that formed on the metallic surface.

KEY WORDS: directional radiative surface properties; emittance; optical properties; oxidized aluminum; spectral directional radiative properties.

1. INTRODUCTION

Emittance is an important radiative property that facilitates pyrometric measurements and numerous thermal computations. The emittance of the opaque surface of a material is generally defined as a ratio of spectral, directional intensity that leaves the surface in a particular direction, at a given temperature and wavelength, and the spectral directional intensity that leaves a blackbody cavity (hohlraum) at the same temperature

[1] Mechanical/Materials Engineering Department, Auburn University, Auburn, Alabama 36849-5341, U.S.A.
[2] To whom correspondence should be addressed. E-mail: teodoge@auburn.edu

and wavelength. Accurate prediction of the behavior of pure aluminum at high temperature in air depends on a knowledge of its radiative properties such as emittance, which depends upon surface roughness, composition, contamination, oxidization, aging, temperature, wavelength, and direction. Numerous radiation heat transfer numerical models accept surface emittance, which accounts for spectral and directional variations. Such models allow a more detailed computation of radiative heat transfer than using total hemispherical properties.

The radiative properties of high-purity thermally oxidized aluminum have been reported in a number of studies [1–4]. Randolph and Overholzer [1] report oxidized aluminum total emissivity measurements at 473, 673, and 873 K. The aluminum samples used in the experiment had a disc shape and were cleaned and polished before mounting. The total emissivity was found to slightly increase with temperature from 0.113 at 473 K to 0.192 at 873 K for an initially polished aluminum sample. Reynolds [2] presents a more careful study of the spectral emissivity of various aluminum surfaces under different heat treatments. The thin-walled cylindrical specimens used were formed from extruded commercial-purity aluminum (99.7%). The measurements were performed at temperatures between 473 and 813 K for a spectral range between 1 to 14 μm. The radiation was collected at 15° from the normal to the sample surface, and the estimated uncertainty was ±20% for polished aluminum and ±10% for roughened and oxidized aluminum over the spectral range from 2 to 10 μm and lower outside. Conroy et al. [3] performed spectral emissivity measurements of 99.99% aluminum at 413 and 623 K, chemically treated to produce a 20 Å aluminum oxide layer. The samples used had a square shape, and a broad band at 980 cm^{-1} (10.2 μm) was observed for emissivity at 623 K due to an amorphous aluminum oxide film. A significant amount of noise was seen in emissivity spectral data for the spectral range between 1900 and 1400 cm^{-1} (5.2–7.1μm). Edwards and Catton [4] present the spectral normal emittance of 1100 aluminum sandblasted with different micron-sized particles. The normal emittance was determined from reflectance measurements, and normal reflectivity measurements were performed at 25° from the sample normal. The sample temperature was about 305.4 K and the spectral normal emissivity varied greatly with surface roughness. Although there is qualitative agreement among reported data, there is a significant deviation among them and none of them report full directional distributions of the emittance of oxidized aluminum and a study of the oxide layer grown.

The objective of this work is to determine the full directional emittance of thermally oxidized 99.99% aluminum with a known surface roughness as opposed to normal at temperatures below its melting point,

using a Perkin–Elmer Spectrum GX (FTIR) spectrometer and to study the oxide layer thickness and composition using Auger electron spectroscopy, X-ray photoelectron spectroscopy, and Auger depth profiling. The FTIR spectrometer provides rapid and accurate detection and processing of the signal. Fourier transform spectrometers have the capability to modulate their radiation source. The spectrometer's detector is sensitive only to modulated radiation. Considering that there is a unique modulation frequency for each source frequency, the FTIR spectrometer allows simultaneous frequency detection and eliminates the need for chopping. A knowledge of such thermophysical property data is a key element in advanced heat transfer computational method development, which accounts for full variation of emittance with direction, wavelength, and temperatures below melting.

2. EXPERIMENTAL APPARATUS

The aluminum sample was mounted on a temperature controlled heater block. Figure 1 shows a schematic of the experimental setup. The

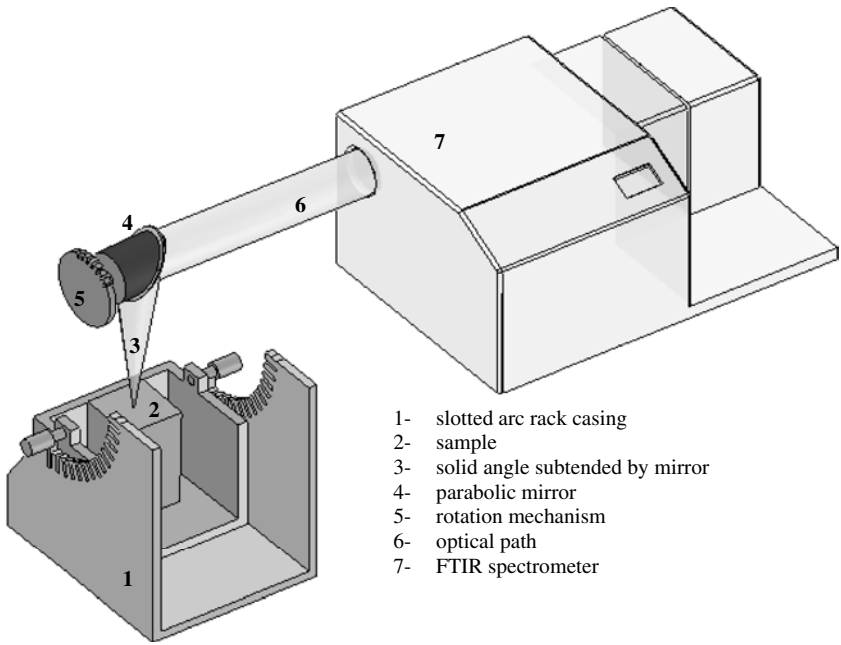

Fig. 1. Schematic of experimental setup.

heater block and the sample are heavily insulated up to the plane of the sample surface. The heater block, the sample, and the insulation are contained in a slotted arc rack casing (1). The sample surface temperature was monitored and controlled by a thermocouple that is embedded through the heater into the sample up to a point just beneath the sample-radiating surface. A Perkin Elmer FTIR spectrometer (Spectrum GX) was incorporated into a previous apparatus, capable of making spectral-directional emittance measurements and is more fully described in Refs. 5 and 6. The radiation that leaves the sample (2) is reflected from a gold-coated off-axis parabolic mirror (4) into a collimated beam (6). The collimated beam is then directed into the FTIR spectrometer (7) towards the detector using the external FTIR viewport. The optical path is calibrated using a blackbody cavity, which is positioned at 90° from the sample and can be viewed by rotating the parabolic mirror. The blackbody-radiating cavity was machined into 152 mm diameter copper, insulated by a 76 mm thick ceramic wool blanket, and its wall temperature was kept at the same temperature as the sample surface using a PID temperature controller. By rotating the parabolic off-axis mirror (4) using a rotation mechanism (5) and moving the sample position to a corresponding position on the slotted arc rack, measurements at different angles to the surface normal were achieved.

The experimental setup was tested for accuracy with pure alumina (99.5% provided by Morgan Advanced Ceramics) at 823 K. The data obtained (Fig. 2) showed good agreement with data published by Vader et al. [7]. The data represent an average of three measurements collected at different times.

A sample of pure aluminum plate (99.99%), 75 mm × 75 mm × 6 mm thick, polished smooth, with a nominal surface roughness of 0.635 μm was used in the experiment. The plate was maintained at high temperature for an extended period of time (150 h) to allow formation of oxide, and then radiative emittance measurements were performed. After cooling the sample, the oxide composition was determined by AES and XPS. The oxide layer thermally grown composition consisted of Al_2O_3 and Al, shown by the binding energy of the Al2p feature at 74.9 eV (Al_2O_3 at 74.7 eV) as seen in Fig. 3 and the Al/O peak ratio (which was ~1.5), and the general AES peak shapes, which are similar to the AES signature for stoichiometric Al_2O_3.

The AES depth profile performed on the oxide layer showed an increasing concentration of elemental Al from the surface to the end of the oxide layer and consequently a decrease of oxygen content from the surface to the end of the oxide layer. The thermally grown layer consists of elemental aluminum and aluminum oxide with a thickness of ~290 nm,

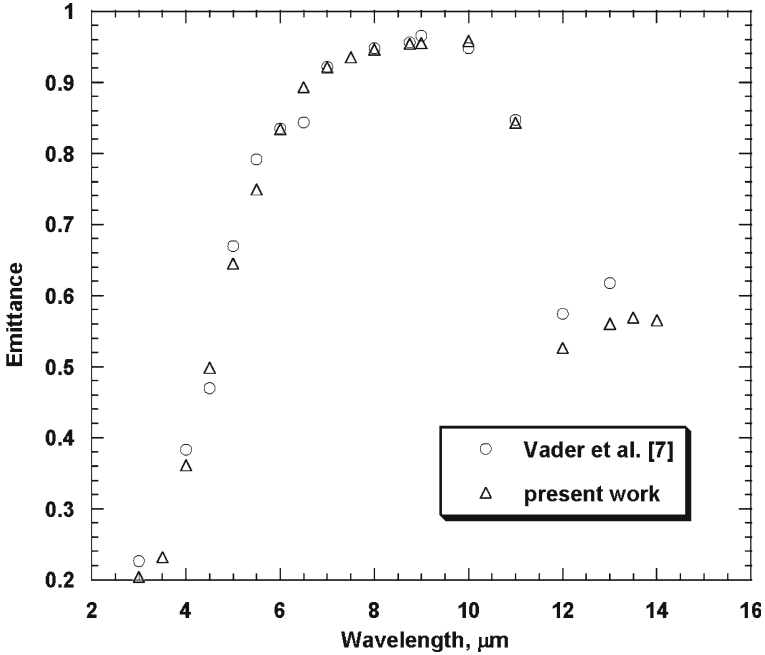

Fig. 2. Comparison of spectral-normal emittance of alumina (99.5%) with Vader et al. [7].

as shown in Fig. 4, which implies that the radiating medium is optically thin.

3. EMITTANCE MEASUREMENTS

The aluminum plate sample was held at 873 K for 150 h to stabilize the effect of oxide on radiative properties. After stabilization, radiation measurements were performed at surface temperatures of 873, 773, and 673 K. Using a 12 mm aperture, the radiation flux was collected over a solid angle of 0.0049 str, which is small enough to assume that the spectral intensity I_λ is constant. All spectral data were averaged over 10 scans using an $8\,\mathrm{cm}^{-1}$ resolution. In order to derive the emittance, the ratio of radiative flux leaving the sample to the radiative flux from the blackbody at the same temperature was determined. Background spectral noise is subtracted from both fluxes. The spectral emittance is calculated from

$$\varepsilon_\lambda(T,\lambda) = \frac{R_s - R_n}{R_{bb} - R_n} \frac{\exp(c_2/\lambda T_s) - 1}{\exp(c_2/\lambda T_{bb}) - 1} \tag{1}$$

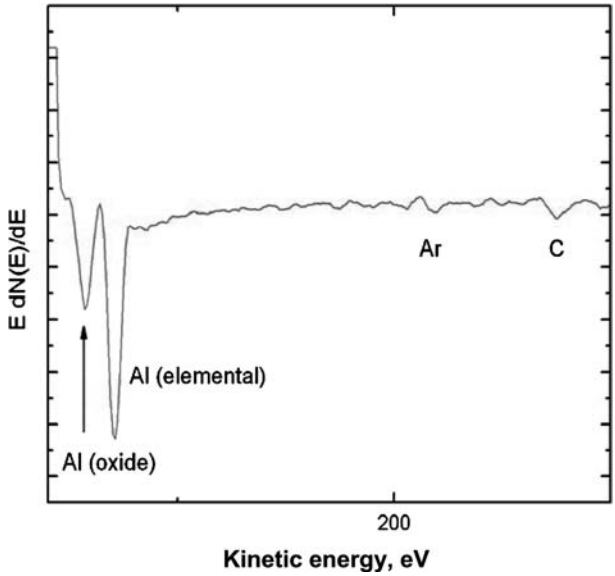

Fig. 3. AES spectrum after 65 min of Ar^+ sputtering.

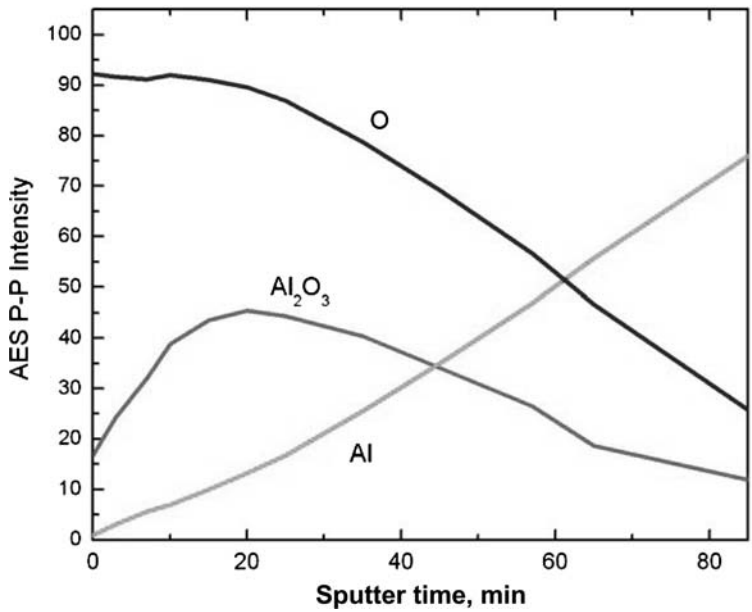

Fig. 4. AES depth profile through the Al film. The Ar^+ sputter rate was 35 Å·min^{-1} measured on a standard thin film of SiO_2.

where R_s is the measured spectral signal obtained from the sample, R_{bb} is the spectral signal obtained from blackbody, and R_n is the background noise signal; T_s is the sample surface temperature, and T_{bb} is the blackbody cavity temperature. The uncertainty in the emittance value $\delta\varepsilon$ is given by [8]

$$\delta\varepsilon_\lambda = \varepsilon_\lambda \frac{\delta T}{\lambda T_s^2} \frac{c_2}{[\exp(-c_2/\lambda T_s) - 1]} \tag{2}$$

where λ is the wavelength and $c_2 = hc_0/k$. According to Eq. (2), the relative uncertainty is inversely proportional to λT_s^2, resulting in a maximum uncertainty at lower temperatures and shorter wavelengths. The temperature uncertainty is comprised of the uncertainty of the blackbody temperature, sample surface temperature, and the stability of the temperature control. Uncertainties for thermocouples used in the experiment reported by manufacturer were 0.4 and 0.05% for temperature control stability. The uncertainty estimation procedure from Ref. 9 was used to determine the total estimated uncertainty as shown in Table I. The maximum uncertainty in the emittance value was found to be less than 3% for the spectral range considered. Reduced spectral-directional emittance data for thermally oxidized aluminum is shown in Table II for surface temperatures of 673, 773, and 873 K.

The data at each wavelength were fit with functions of polar angle (some smoothing was necessary to fit the data beyond 8 μm). These curves were compared to Fresnel's equation [10]:

$$\varepsilon = 1 - \frac{1}{2}\left(\frac{(n\beta - \cos\theta)^2 + (n^2+k^2)\alpha - n^2\beta^2}{(n\beta + \cos\theta)^2 + (n^2+k^2)\alpha - n^2\beta^2} + \frac{\left(n\gamma - \alpha/\cos\theta\right)^2 + (n^2+k^2)\alpha - n^2\gamma^2}{\left(n\gamma + \alpha/\cos\theta\right)^2 + (n^2+k^2)\alpha - n^2\gamma^2}\right) \tag{3}$$

Table I. Uncertainty Estimates of the Emissivity Measurement

Parameter	Estimated $\pm 2\sigma$ confidence limits (%)	Emissivity change at $\lambda = 3\,\mu$m	Emissivity change squared ($\times 10^7$)
Sample surface temperature	0.4	0.0016	25.6
Blackbody temperature	0.4	0.0016	25.6
Stability of the BB temperature	0.05	0.0002	0.4
Stability of sample temperature	0.05	0.0002	0.4
Total uncertainty in emissivity $[\Sigma(\delta\mu_i)^2]^{1/2}$			0.0026
Total % uncertainty in emissivity ($\varepsilon = 0.0944$, at $T = 673$ K)			2.8%

Table II. Measured Spectral-Directional Emittance of Thermally Oxidized Aluminum at 673 K (1st row), 773 K (2nd row), and 873 K (3rd row)

	Polar angle (deg)						
λ(μm)	0°	12°	24°	36°	48°	60°	72°
3	0.094	0.108	0.104	0.109	0.118	0.120	0.135
	0.121	0.137	0.137	0.142	0.150	0.168	0.161
	0.152	0.163	0.166	0.173	0.184	0.211	0.206
4	0.098	0.113	0.106	0.110	0.116	0.129	0.135
	0.117	0.132	0.131	0.136	0.144	0.162	0.162
	0.141	0.151	0.153	0.159	0.169	0.196	0.199
5	0.099	0.109	0.105	0.107	0.112	0.126	0.137
	0.112	0.126	0.124	0.128	0.137	0.155	0.163
	0.132	0.141	0.142	0.147	0.158	0.184	0.198
6	0.098	0.106	0.104	0.105	0.111	0.125	0.147
	0.107	0.120	0.118	0.123	0.131	0.150	0.169
	0.125	0.132	0.132	0.138	0.148	0.175	0.204
7	0.097	0.105	0.101	0.103	0.108	0.125	0.158
	0.105	0.116	0.114	0.118	0.127	0.146	0.181
	0.122	0.126	0.126	0.131	0.142	0.169	0.218
8	0.096	0.103	0.100	0.102	0.107	0.124	0.160
	0.103	0.112	0.110	0.115	0.123	0.144	0.183
	0.118	0.121	0.121	0.126	0.137	0.166	0.220
9	0.106	0.115	0.113	0.119	0.129	0.154	0.193
	0.111	0.121	0.122	0.130	0.145	0.173	0.212
	0.125	0.129	0.131	0.140	0.157	0.193	0.244
10	0.101	0.109	0.109	0.116	0.128	0.157	0.205
	0.107	0.116	0.117	0.126	0.143	0.177	0.224
	0.120	0.122	0.125	0.135	0.154	0.195	0.255
11	0.107	0.120	0.135	0.160	0.200	0.265	0.319
	0.114	0.127	0.143	0.175	0.225	0.296	0.344
	0.126	0.135	0.155	0.191	0.247	0.326	0.376
12	0.099	0.108	0.110	0.119	0.139	0.181	0.237
	0.101	0.109	0.113	0.128	0.153	0.197	0.253
	0.114	0.114	0.122	0.137	0.166	0.217	0.285
13	0.095	0.104	0.106	0.110	0.128	0.162	0.219
	0.100	0.105	0.108	0.119	0.139	0.174	0.233
	0.111	0.110	0.115	0.126	0.149	0.191	0.265
14	0.097	0.102	0.106	0.106	0.124	0.154	0.213
	0.098	0.103	0.104	0.114	0.130	0.163	0.225
	0.109	0.106	0.110	0.119	0.138	0.179	0.255

$$\alpha^2 = \left(1 + \frac{\sin^2\theta}{n^2+k^2}\right)^2 - \frac{4n^2}{n^2+k^2}\left(\frac{\sin^2\theta}{n^2+k^2}\right) \tag{4}$$

$$\beta^2 = \frac{n^2+k^2}{2n^2}\left(\frac{n^2-k^2}{n^2+k^2} - \frac{\sin^2\theta}{n^2+k^2} + \alpha\right) \tag{5}$$

$$\gamma = \frac{n^2-k^2}{n^2+k^2}\beta + \frac{2nk}{n^2+k^2}\left(\frac{n^2+k^2}{n^2}\alpha - \beta^2\right)^{\frac{1}{2}} \tag{6}$$

in order to identify the real and imaginary parts of the spectral complex index of refraction using a secant iteration method. The refractive index n is shown in Fig. 5 to increase with temperature and wavelength. Between 3 and 8 μm the refractive index n increases slightly with temperature and wavelength, and increases more significantly beyond 8 μm. The extinction coefficient k is seen to increase with wavelength and temperature as shown in Fig. 6.

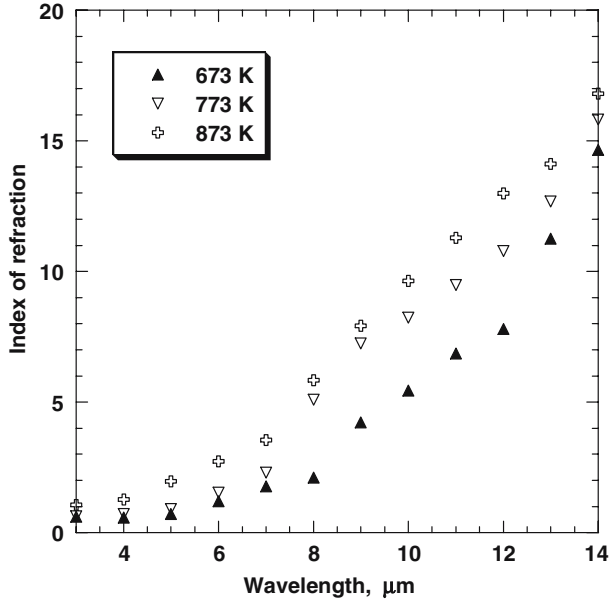

Fig. 5. Spectral refractive index at 673, 773, and 873 K.

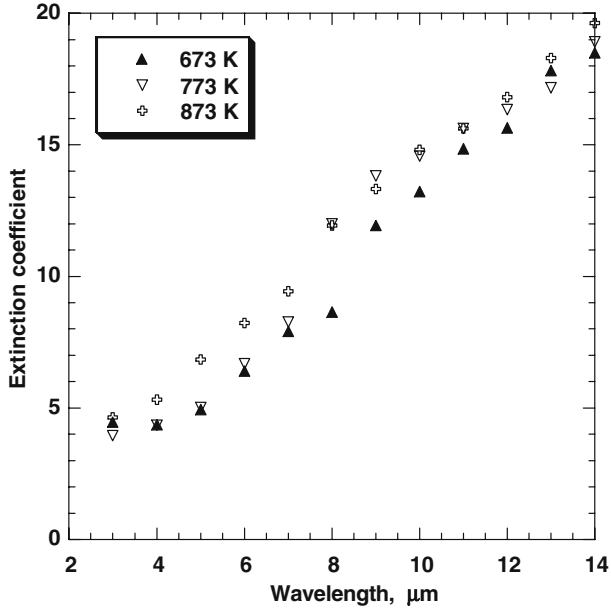

Fig. 6. Spectral extinction coefficient at 673, 773, and 873 K.

4. DISCUSSION

Spectral-normal emittance data from Reynolds [2] and Conroy et al. [3], together with the present data, are shown in Fig. 7. Even though the data from Refs. 2 and 3 are in the same spectral region, there is not good agreement between them. The data from Ref. 2 give both the spectral emissivity of 99.7% polished aluminum at 697 K and the spectral emissivity of 99.7% roughened aluminum at 599 K after various heat treatments. Here, the effect of surface roughness clearly dominates the emittance increase over the temperature effect. The measured values of spectral-normal emittance from the present work are higher than values reported in Ref. 2 for a polished sample, and this is probably due to higher surface roughness. Similar trends are observed in both data.

The data from Ref. 3 come from a 99.99% aluminum sample measured in air with a surface roughness of 0.762 μm, which was cleaned in a chrome/phosphoric acid solution in order to obtain a 2 nm thickness of consistent, uniform barrier aluminum oxide layer. The measurement was performed at 623 K. In spite of 24 degree temperature measurement difference, there is some agreement between data from the roughened sample in Ref. 2 and the chemically treated sample in Ref. 3. Comparing the

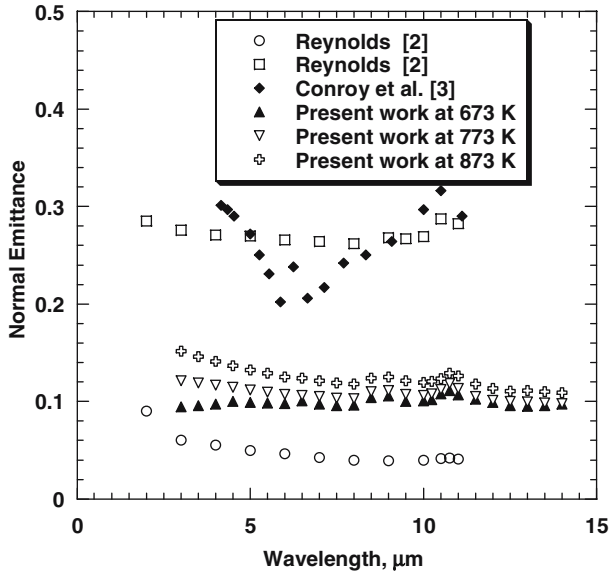

Fig. 7. Spectral normal emittance of oxidized aluminum at 673, 773, and 873 K.

spectral normal emittance from the present work with the data from Ref. 3, there is an obvious difference even though the samples used have very close surface roughness—0.635 μm in present work and 0.762 μm in Ref. 3. The difference can be explained by taking into account the sample compositions. The aluminum sample used in Ref. 3 was chemically treated to produce a uniform barrier oxide of approximately 2 nm, whereas further Auger electron spectroscopy performed on the present samples revealed that the thermal layer grown on the sample surface is comprised of pure aluminum and aluminum oxide and has a thickness of about 290 nm. This explains the higher emittance observed on samples in Ref. 3 due to the influence of greater aluminum oxide properties of the consistent and uniform barrier layer. Unfortunately, the formed oxide layer composition is not addressed in both Refs. 2 and 3.

The spectral-normal emittance data from the present work, is seen to increase slightly with temperature as shown in Fig. 7. The two slight peaks observed at 8.5 and 11 μm were attributed to aluminum oxide grown on the sample surface.

Figure 8 shows the spectral-normal emittance from the present work, together with data from Bauer et al. [11]. The sample used in Ref. 11 is an Al 5754 alloy (polished) that contains at least 95.7% aluminum.

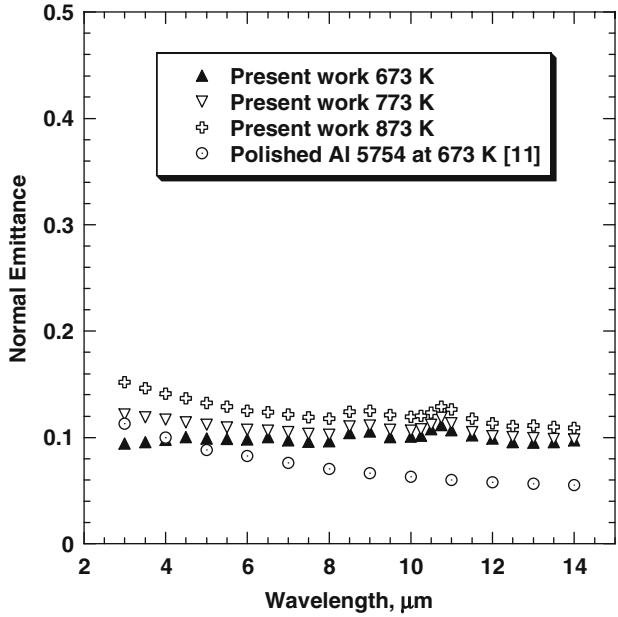

Fig. 8. Spectral normal emittance comparisons.

The measurements were performed in vacuum and a protective gas atmosphere to avoid oxidation. From Fig. 8, it can clearly be observed that the spectral normal emittance from Ref. 11 does not exhibit any peak between 8 to 12 μm and normal emittance decreases smoothly with wavelength for the spectral range considered, suggesting a pure metallic behavior. The data from the present work at 673 K agree qualitatively with data from Ref. 11 even though the emittance value is higher beyond 5 μm. The explanation is supported by the presence of aluminum oxide that not only slightly increases the emittance but also develops two slight peaks as mentioned above. Moreover, the surface roughness of samples used in the present work is higher than that of the polished sample from Ref. 11.

Figure 9 shows the present measurements of the directional emittance of Al oxidized at high temperatures below its melting point at a wavelength of 3 μm. The directional emittance is seen to increase slowly with polar angle up to 36° and more greatly thereafter until grazing, suggesting a metallic behavior. Generally, the directional emittance is seen to slightly increase with temperature. Figure 10 presents the directional emittance of oxidized aluminum at 673 K at wavelengths of 9, 10, and 11 μm. Here, at higher wavelengths the emittance is seen to increase with polar angle

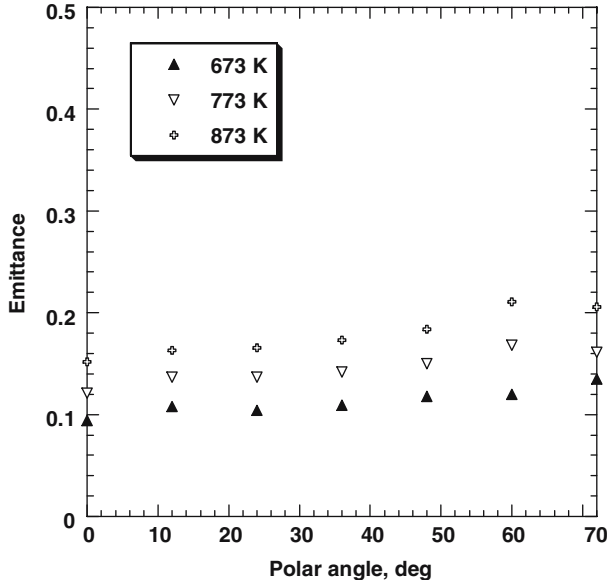

Fig. 9. Directional emittance of oxidized aluminum at 3 μm as a function of temperature.

from normal to 72°. Here the behavior at 11 μm should be noted, near around where a maximum of the normal emittance is seen. At a wavelength of 11 μm, the directional emittance increases sharply with polar angles beyond 24° until 72° as compared with wavelengths of 9 and 10 μm. This behavior can be probably explained by the presence of aluminum oxide in the 290 nm layer grown by heating. Then, the appearance of aluminum oxide into elemental aluminum gives not only a couple of slight peaks in normal emittance but also alters the directional behavior around the spectral range where the peaks were developed. This influence is seen to increase with temperature.

5. CONCLUSIONS

The spectral-directional emittance of high purity (99.99%) aluminum, thermally oxidized in air at temperatures between 673 to 873 K, is determined from measurements of the radiative intensity leaving the specimen. An AES spectrum performed after cooling the sample shows that the oxidized layer is composed of aluminum and aluminum oxide. An AES depth

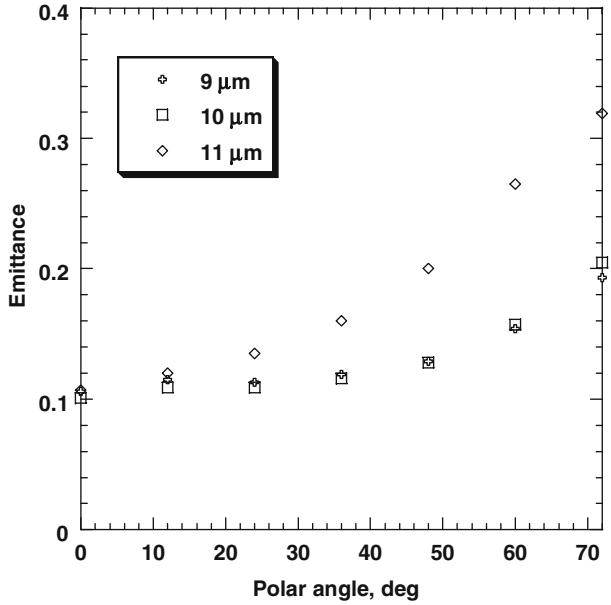

Fig. 10. Directional emittance of oxidized aluminum at 673 K at 9, 10, and 11 μm.

profile indicates that the amount of elemental aluminum increases with depth, and the amount of oxygen decreases with depth and vanishes when the aluminum substrate is reached. The normal spectral emittance of oxidized aluminum is seen to increase slightly with temperature and decrease with wavelength between 3 and 8 μm and beyond 11 μm. Between 8 and 11 μm two slight peaks appeared due to the aluminum oxide influence. The thermally oxidized aluminum is seen to exhibit a directional emittance in good agreement with theoretical predictions for metals for wavelengths between 3 and 8 μm. Beyond 8 μm, the influence of aluminum oxide is seen to dominate the directional emittance and good agreement with Fresnel's equation was not found. The complex refractive index was determined after smoothing the data above 8 μm.

ACKNOWLEDGMENT

The authors gratefully acknowledge financial support received from NASA's Space Product Development Program at Marshall Space Flight Center under Cooperative Agreement No. NCC8-240.

REFERENCES

1. C. P. Randolph and M. J. Overholzer, *Phys. Rev.* II **2**:144 (1913).
2. P. M. Reynolds, *J. Appl. Phys.* **12**:111 (1961).
3. C. M. Conroy, J. G. Guthrie, A. J. Sharkins, B. J. Sparr, R. A. Crocombe and R. Curbelo, *Appl. Spectrosc.* **41**:688 (1987).
4. D. K. Edwards and I. Catton, in *Advances in Thermophysical Properties at Extreme Temperatures and Pressures*, *Proc. 3rd Symp. Thermophys. Props*. (West Lafayette, Indiana, 1965), pp. 189–999.
5. P. D. Jones, G. Teodorescu, and R. A. Overfelt, presented at *ASME Summer Heat Transfer/Fluids Eng. Conf.* (Charlotte, North Carolina, 2004).
6. P. D. Jones, D. E. Dorai-Raj, and D. G. McLeod, *J. Thermophys. Heat Transfer* **10**:343 (1996).
7. D. T. Vader, R. Viskanta, and F. P. Incropera, *Rev. Sci. Instrum.* **57**:87 (1985).
8. W. M. Branderberg and O. W. Clausen, *Int. Aeros. Abstr.* **4**:313 (1964).
9. R. J. Moffat, *Exp. Therm. Fluid Sci*. **1**:3 (1998).
10. R. Siegel and J. Howell, *Thermal Radiation Heat Transfer* (Taylor and Francis, New York, 2002).
11. W. Bauer, H. Oertel and M. Rink, paper presented at *15th Symp. Thermophys. Props.* (Boulder, Colorado, 2003).